Meso-Scale FEA Modeling to Simulate Crack Initiation and Propagation in Boron Steel

Yijung Chen, Omar Faruque, Cedric Xia, Alex Akkerman, Dennis Lam
Ford Motor Company

Abstract

*The scope of this paper focuses on the characterization and prediction of potential crack initiation and propagation in a boron-steel component under extreme impact load, utilizing a meso-scale FE (0.2 mm solid element) modeling with the MIT MMC (modified Mohr-Coulomb) fracture criterion. The MMC fracture criterion is implemented through LS-DYNA® *MAT224 and *MAT_ADD_EROSION with GISSMO option. A finite element mesh with total number of elements close to 100 million is created to investigate the accuracy of MMC criterion in predicting fracture of a boron component in a dynamic impact test. The CAE results are compared to sled test results for system force-deflection, part deformation mode and crack initiation and propagation.*

Introduction

As vehicle manufacturers continue efforts to reduced overall vehicle weight, the application of ultra-high strength steels in automotive design is expanding because these materials provide the required strength while enabling lighter-weight components. . These materials demonstrate some unique characteristics during extreme high load due to lesser ductile characteristics. In a typical passenger vehicle, the B-pillar, which is the middle vertical column between two side doors, is a major load-carrying structure for its upper body. A CAE investigation was conducted to simulate a vehicle B-pillar subsystem when it is subjected to severe impact force. In the reference example, the B-pillar is made out of hot-stamped, press-hardened boron steel. Under extreme load, the boron component may crack.

This type of failure is microscopic in nature. In order to capture the mechanical behavior correctly, we proposed to model the component at meso-scale level with solid elements. Currently, modeling with shell elements is the main stream practice in crash safety simulation. The kinematic assumptions – Kirchhoff or Mindlin – enable the simplification of continuum mechanics and give rise to shell element formulations. Through the years, the shell modeling has adequately provided reliable predictions of structural stiffness. With the enhancement of the material model, it also gives a good indication of potential material failure. However, to predict crack initiation and propagation in detail, we need a modeling methodology with fine solid elements.

We also incorporate a recent development in material fracture modeling from the MIT fracture consortium. An in-depth study of its application in boron steel is given in a sister paper[2] by ArcelorMittal Global R&D team. In our example problem, the boron B-pillar is modeled with 0.2 mm size solid elements. The superfine mesh of the B-pillar increases the model size to almost 100 million elements – a model size that is probably one of the largest crash models

available today. Such large scale model also pushes the limits of hardware and software. In another LS-DYNA paper [1], team provides a detail description of the challenges and their remedies.

Meso vs. Macro and Solid vs. Shell

Meso-scale is an intermediate range between macro-scale and micro-scale. For steel applications, the meso-scale can be defined by the steel grain sizes, which are in the range of 100μm. For practical purposes, the MIT fracture consortium recommended a mesh size of 0.2mm (200μm) as a minimum for steel meso-scale modeling. One major rationale for advocating meso-scale modeling is to eliminate the mathematics approximation in current crash safety simulations – mainly the shell approximation. A shell is an approximation of continuum mechanics for a thin layer structure. This approximation enables the development an efficient simulation tool in macro-scale to study crash events. The approximations are in the shell's thru-thickness or out-of-plane direction. They simplify the shell cross-section kinematics, approximate the thru-thickness stress and cross-section shear. These approximations provide a good foundation to develop the stiffness matrix of structure. By increasing the thru-thickness integration points, one can increase the resolution to monitor the progress of damage.

Solid elements are recommended by the MIT fracture consortium for meso-scale sheet metal modeling. The 0.2mm mesh size guideline is sufficient to model the thru-thickness with 8 layers for most crash safety critical structures. Figure 1 illustrates a local solid mesh of such a model alongside with its shell mesh representation. When stress in an element reaches its element erosion state, meso-scale solid model will remove element. This step will form a cut (surface) or void (internal) and create a local stress concentration or even singularity within the model (color red), which may propagate either in thru-thickness or in-plane direction. Unlike its shell approximation counterpart, it can only suppress one of its (Gaussian) integration point, weakening the structure locally but not enough to create geometrically singular feature. Therefore, it is reasonable to infer that a meso-scale solid element modeling approach can help us capture the true mechanism of crack propagation in steel, which is a sequence of singularity events.

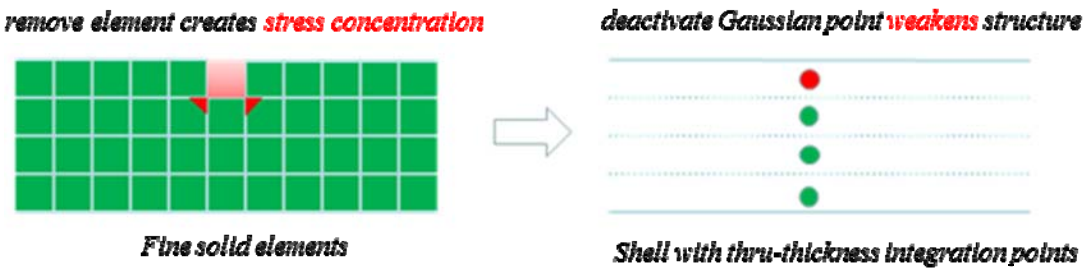

Fig. 1 Solid vs. Shell – Reality vs. Approximation

The meso-scale modeling results in large model size. A typical vehicle B-pillar with mesh size of 8mm shell element will generate a 5000-element model. A 2mm shell will be 10,000+ elements. For a meso-scale modeling, 0.2mm solid element will create a 100M-element model. It requires

that the time step be dropped to 5E-05 ms or lower with mass scaling active. With this setting we can limit the percentage of added mass to less than 3%.

For such a fine solid element modeling, LS-DYNA requires a segment-based contact for the analysis to execute properly. This requires the SOFT parameter set to 2 in the general *CONTACT keyword.

MIT MMC Fracture Criterion and LS-DYNA Implementation

The meso-scale modeling in this paper incorporates the MMC (Modified Mohr-Coulomb) fracture criterion proposed by the MIT fracture consortium [3-5]. The proposed MMC fracture criterion in the form of strain space can be expressed as

$$\left\{\frac{A}{c_2}\left[c_3+\frac{\sqrt{3}}{2-\sqrt{3}}(1-c_3)\left(\sec\left(\frac{\bar{\theta}\pi}{6}\right)-1\right)\right]\left[\sqrt{\frac{1+c_1^2}{3}}\cos\left(\frac{\bar{\theta}\pi}{6}\right)+c_1\left(\eta+\frac{1}{3}\sin\left(\frac{\bar{\theta}\pi}{6}\right)\right)\right]\right\}^{-\frac{1}{n}} \quad \text{Eq. (1)}$$

This formula forms an analytical boundary to define fracture surface. Two variables, η the stress triaxiality and $\bar{\theta}$ the normalized Lode angle, are defined as

Stress triaxiality
$$\eta=\frac{-p}{\sqrt{3J_2}}=\frac{\sigma_m}{\bar{\sigma}_{Mises}} \quad \text{Eq. (2)}$$

Lode angle
$$\theta=\frac{1}{3}\cos^{-1}\left(\frac{3\sqrt{3}}{2}\frac{J_3}{J_2^{3/2}}\right) \qquad 0\le\theta\le\frac{\pi}{3} \quad \text{Eq. (3)}$$

Normalized Lode angle
$$\bar{\theta}=1-\frac{6\theta}{\pi} \qquad -1\le\bar{\theta}\le 1 \quad \text{Eq. (4)}$$

where p is hydrostatic stress, J_2 and J_3 second and third invariants of stress deviator tensor, σ_m is mean stress and $\bar{\sigma}_{Mises}$ denotes von Mises stress. The required coefficients, namely A, c_1, c_2, c_3 and n, can be derived from curve-fitting of available material test data.

There are two options in LS-DYNA to implement MMC fracture criterion without involving user subroutine. The first choice is *MAT_TABULATED_JOHNSON_COOK (*MAT224). It provides tabulated input for plastic failure strain versus stress triaxiality in different Lode angles. It is worth noting that the sign of stress triaxiality in *MAT224 is reversed compared to the conventional definition. In this paper, the MMC fracture criterion is used as response surface to generate data table (functions) as *MAT224 input. There are two shortcomings of applying *MAT224 in general practice. Firstly, as the name implies, it can only use the fracture criterion in conjunction with JOHNSON_COOK material modeling. Even though it has an option to use tabulated functions as input, it is still limited to an isotropic plasticity model. Secondly, it doesn't provide true damage evolution. The NUMINT parameter can provide an approximation of damage evolution through failure of integration points, but it is only available in shell formulation and won't be meaningful for a solid element because of the choice of one-point integration in auto applications.

An alternative implementation of the MMC fracture criterion is through GISSMO, which is an option under *MAT_ADD_EROSION with IDAM=1. GISSMO provides its own analytical form of fracture surface. To implement the MMC fracture criterion in GISSMO, we generate a matrix (stress triaxiality and Lode angle) of data from MMC and curve-fits the GISSMO coefficients from this set of pseudo-test data. By doing so, we force the GISSMO to behave like MMC. The GISSMO provides an algorithm for damage evolution. It also can work with any choice of material model. In this paper, we use *MAT_PIECEWISE_LINEAR_PLASTICITY (*MAT24) to model boron steel.

More in-depth description of the development of MMC LS-DYNA material cards is provided in another LS-DYNA paper [2].

CAE Model Description

The model used in this project is a side impact sled test model as shown in Figure 4. The B-pillar is attached to the rocker and to the roof rail. A customized fixture is used to mount the B-pillar subsystem, which is constrained at both ends of the rocker and the roof rail. The key components in the models are the rocker, extending from A-pillar to C-pillar, B-pillar inner, honeycomb blocks to stop the sled, barrier face with special design, roof rail and brackets, honeycomb supports behind the rocker, and B-pillar outer. Except the B-pillar outer, the components listed are modelled with shell elements with element size range from 1.0 mm to 5.0 mm.

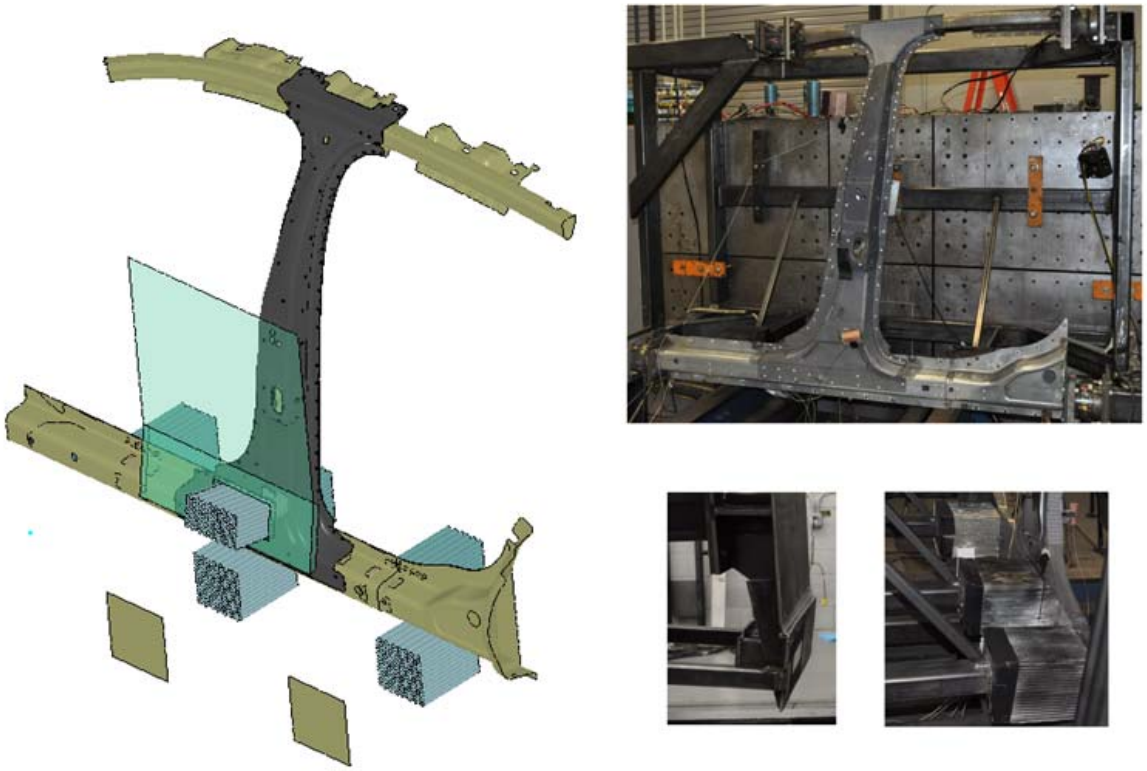

Fig. 4 Sled CAE model and Test Setup

The B-pillar outer, which is made with boron steel, received special treatment in meshing. It is modeled in meso-scale with solid element size in the range of 0.2mm. The resultant CAE model has just less than 100M elements including about 500K shell elements used for modeling the rocker, roof rail and B-pillar inner components and honeycomb blocks. Spotwelds that join parts together are modeled with beam elements except spotwelds that join the meso-scale modeled part (the B-pillar outer) to other parts. This group of spotwelds is modeled with solid elements with tied contact as shown in Figure 5.

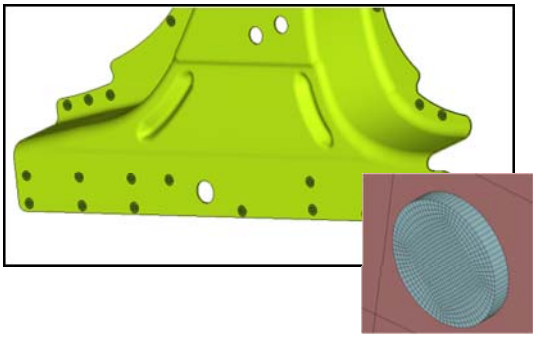

Fig. 5 Solid Spotweld Nugget Model

Enhanced Spotweld and HAZ Modeling

The main motivation to model the spotwelds joining the meso-scale B-pillar to other parts with very fine solid elements is to capture the right spotweld failure mechanism. We also need to model the Heat Affected Zone (HAZ) as shown in Figure 6.

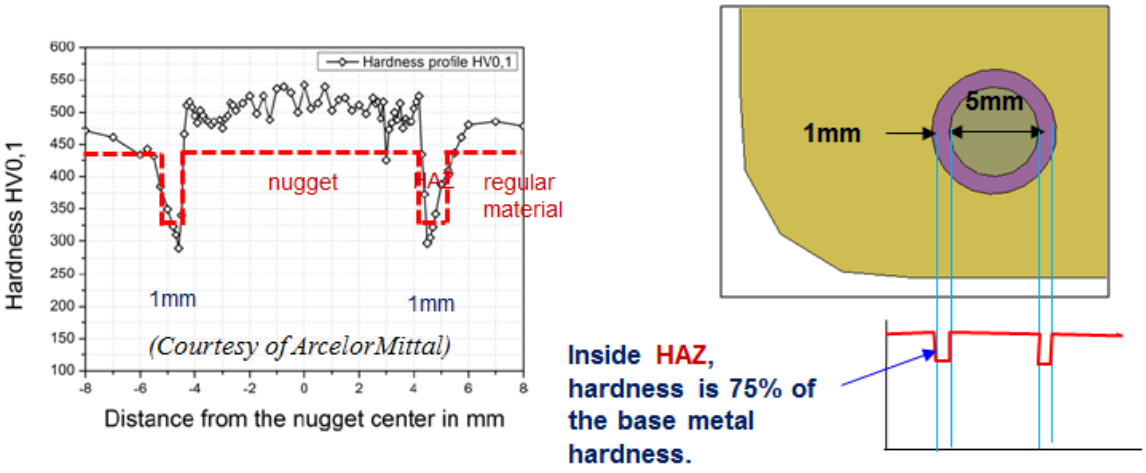

Fig. 6 HAZ Modeling

As many researchers have found, material behavior can be altered by the extreme heat generated during welding. The left side of Fig. 6 taken from the work of Burget and Sommer [6] shows the

hardness profile across a typical resistant spotweld or arc spotweld. The strength in a narrow region, the heat affected zone, can be reduced as much as 50 percent across the narrow zone. In our model, the narrow zone around the spotweld nugget has a width of 1 mm, which seems to be a good realistic representation. The right side of Figure 6 shows our spotweld model specification – 5mm nugget diameter, 1mm HAZ width, and material softening parameter of 0.75, which is an averaged value across the narrow heat affected zone.

Pre- and Post-processing Requirements

In preparing the meso-scale model, we quickly learned that the traditional hardware and software are inadequate to handle the preprocessing and post-processing. While we didn't investigate deliberately the minimum hardware requirement to handle the 100 million element model, we found that a system with memory size greater than 100GB was required to load the 100 million element model. We also learned that a simple command of rotating the model to a different angle took several minutes – a manipulation that is expected to be instantaneous in an interactive environment. A command in LS-PrePost® to plot plastic strain or other flange values took several hours to finish just one state. The response time to interrogate such a large model is so long that much of the preprocessing and post-processing was carried out in batch mode with command files and customized scripts. While we could still assess and interpret the analysis results with this time consuming process, it is not feasible to apply as common practice.

CAE Results and Test Comparison

In Figure 7, we compare the CAE result and test data for the moving sled in acceleration, velocity and displacement. Red lines are from the test while blue lines are generated from the CAE. The comparison shows a good correlation between CAE and test.

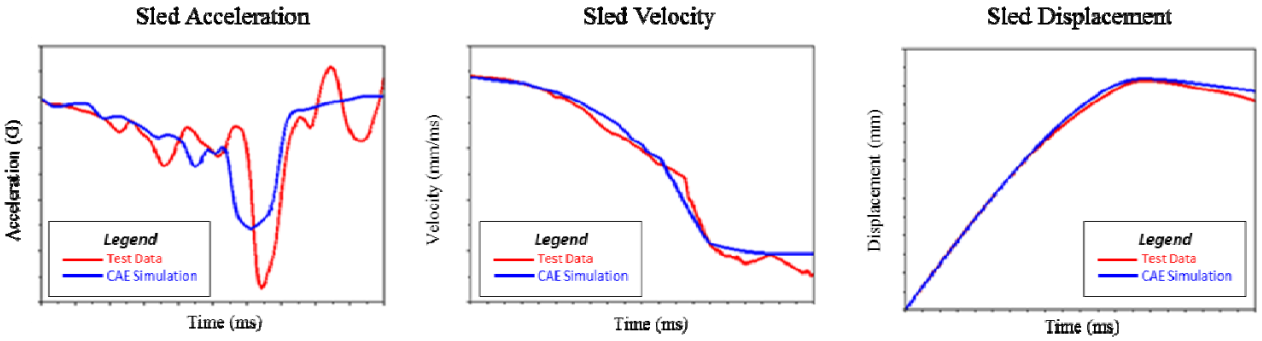

Fig. 7 Test vs. CAE – Acceleration, Velocity and Displacement

Figure 8 shows the comparison of deformed shape from CAE to test results, which also shows good correlation. . At the top portion of B-pillar outer, spotwelds on the flanges of both sides separate and subsequently cracks initiated from the separated spotwelds and propagate toward the center of the B-pillar. At the bottom, the spotwelds separated and caused the B-pillar outer to separate from the rocker and B-pillar inner.

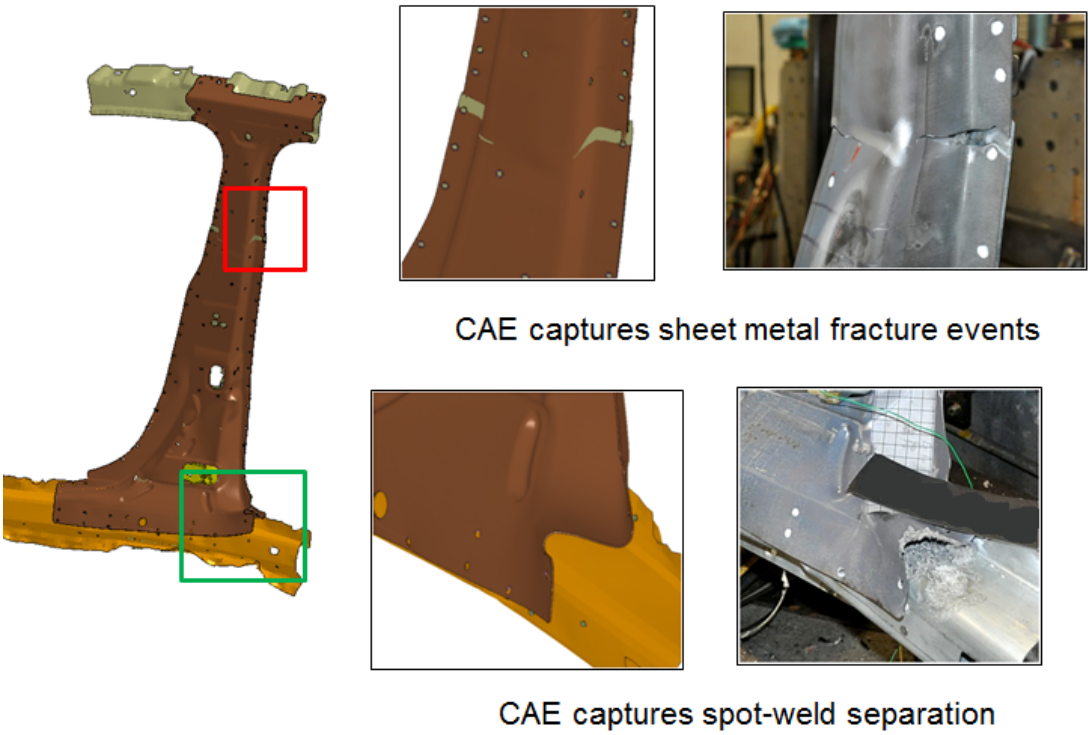

Fig. 8 Test vs. CAE – Deformation mode, spotweld peeling and material rupture

The detailed animations of spot-weld rupture reveal the sequence of spotweld rupture – which go in the thru-thickness direction first, then go in the circumferential direction later. In the top portion of B-pillar, the material erosion in HAZ forms a semi-circle in just 1ms. The process pauses 5ms, then under the influence of structural bending, both ends of semi-circle become crack initiation points and propagate the crack into center of B-pillar section. At the bottom of B-pillar, the material erosion in HAZ continued in shear and peeled out the whole segment of material surrounding the spotweld nuggets that led to separation of two layers. Both events were not observable in the high speed video (time interval=1ms). Only CAE animation made this observation possible.

The GISSMO gives better prediction in terms of the number of spotwelds peeling off at the bottom of the B-pillar. The *MAT224 predicts more spotwelds peeling off than test results. The difference may due to the contribution from damage evolution. With the damage evolution option in GISSMO active, some spotwelds can stay intact longer.

Conclusions and Next Steps

We demonstrated the possibility to characterize material fracture such as spotweld separation, crack initialization and crack propagation using a meso-scale model. The modeling of HAZ proves to be a crucial step in test correlation.

In the process of building this large scale model, we exposed a few issues in hardware and software for handling large scale problems. The required pre- and post-processing tools are now functional and we successfully completed the project. However, higher performing graphics capabilities are required to be able to build the model and process the results without lengthy delays.

The *MAT224 can be further enhanced by adding damage evolution. But for current CAE applications, adding an advanced material fracture criterion in *MAT_ADD_EROSION, such as GISSMO, should be an effective approach. However, an effort to implement the general fracture criterion with tabulated input and the feature of damage evolution feature should be considered.

Acknowledgements

We would like to thank Dr. Min Kuo, Mr. Michael Lizak, Dr. Sriram Sadagopan, Dr. Gang Huang and Dr. Hong Zhu of ArcelorMittal Global R&D for their support of this project.

References

1. A. Akkerman, Y. Chen, B. El-Fadl, O. Faruque and D. Lam, “LSDYNA performance in side impact simulations with 100M element models”, 13th International LS-DYNA Users Conference 2014, Dearborn, Michigan
2. G. Huang, H. Zhu, S. Sriram, Y. Chen, Z. C. Xia, O. Faruque, “Fracture Prediction and Correlation of AlSi Hot Stamped Steels with Different Models in LS-DYNA”, 13th International LS-DYNA Users Conference 2014, Dearborn, Michigan
3. Wierzbicki, T.; Bao, Y.; Lee, Y. and Bai Y., “Calibration and evaluation of seven fracture models,” International Journal of Mechanical Sciences, vol. 47, 719-743, 2005.
4. Bai, Y. and Wierzbicki, T., “A new model of metal plasticity and fracture with pressure and Lode dependence,” International Journal of Plasticity, 24, 1071–1096, 2008.
5. Bai, Y. “Effect of Loading History on Necking and Fracture,” PhD thesis, Massachusetts Institute of Technology, 2008
6. S. Burget, and S. Sommer, “Characterization and modeling of fracture behavior of spot welded joints in hot-stamped ultra-high strength steels”, 11th LS-DYNA Forum, 2012, Ulm, Germany.